Volume 8 | Issue 1 Article 3

2019

Methanol Masers in Star-Forming Regions

Nicolas Clarisse
DePaul University, nclarisse26@gmail.com

Anuj P. Sarma
asarma@depaul.edu

Methanol Masers in Star-Forming Regions

Acknowledgements

ACKNOWLEDGEMENTS I would like to thank DePaul University's College of Science and Health for providing the financial means and the great opportunity to partake in the Undergraduate Research Apprentice Program. I'd also like to thank Dr. Sarma for letting me be a part of his research and guiding me through this process and for the exposure to cutting edge physics outside the classroom, which I will continue to pursue.

Methanol Masers in Star-Forming Regions

Nicolas Clarisse*
Department of Chemistry
Dr. Anuj Sarma
Department of Physics

ABSTRACT Methanol molecules in star-forming regions emit detectable microwave radiation. In particular, the rotational energy state transitions of methanol are responsible for two types of masers: Class I and Class II, found in the bipolar outflows and accretion disks of star-forming regions, respectively. Masers, being intense point-like sources in our sky, serve as an excellent source of information in further understanding the environment of high-mass star-forming regions due to their intense luminosities. High-mass star formation is still not entirely understood and remains an observational challenge. We have compiled a list of all the methanol maser transitions observed in the literature, in order to provide a small-scale database that can be used to study the morphology of maser distribution, and as a source to plan for observation of the Zeeman Effect to measure magnetic fields in star-forming regions.

INTRODUCTION

When we look up at the sky, we see light that comes mostly from a few bright stars. In between these stars lies the interstellar medium, which is comprised of gas (mainly hydrogen, with 10% helium mixed in), and dust (mainly carbon and silicon based). Most of the gas in the interstellar medium exists in the form of atomic or molecular clouds. Star formation follows a process where cores in molecular clouds collapse first under their own gravity to form protostars. Such protostars are always accompanied by an accretion disk, and eject a powerful bipolar stream of gas called an outflow (Max Planck Institute for Astronomy, MPIA). Eventually the protostar accretes enough mass to turn on nuclear fusion in its core and form a star. The general idea of high-mass (eight times the mass of our sun) star formation is akin to that of low-mass stars but their time scale of burning hydrogen is much quicker, which is connected to a high radiative pressure put on the gas collapsing inward due to gravity. Understanding how high-mass stars form is a major focus of current research into star formation, because of their significant impact on the interstellar medium. Several key elements like silicon and iron can only be formed in high-

* nclarisse26@gmail.com
Research Completed Jun – Nov 2018

mass stars. At the end of their lifetimes, high-mass stars kick back these elements into the interstellar medium, enriching it for a new generation of stars. However, observation of high-mass star formation presents a challenge because they are farther away than their low mass counterparts, and usually never form in isolation. Therefore, very high spatial resolution (the ability to discern detail while observing an object) is needed to observe high-mass star formation. An effective way to observe high-mass star formation is by observing masers (Microwave Amplification by Stimulated Emission of Radiation), astronomical sources that resemble the lasers (Light Amplification by Stimulated Emission of Radiation) that we use here on Earth, except that masers lie in the microwave region of the electromagnetic spectrum. Just like lasers, masers occur when a population of molecules (or atoms) is pumped into an upper energy level from which they collapse into a lower energy state; in doing so, they release a large amount of energy in the form of microwave radiation. This pumping into an upper state can occur by radiative (electromagnetic) processes or through collisions (thermal). In particular, methanol masers occur in star-forming regions, and offer an excellent way to observe high-mass star-forming regions with very high spatial resolution because they are strong sources with small spatial extent. Methanol masers form not only in the accretion disks in star-forming regions (in which case they are known as Class II methanol masers), but also in the bipolar outflows (in which case they are known as Class I). The pumping into the upper levels of the energy states of such masers is by collisional excitation for Class I methanol masers and radiative excitation in the infrared for Class II methanol masers.

The presence of a magnetic field in the regions where methanol masers are generated, like in a star-forming environment or gas cloud, causes the electromagnetic radiation produced in those regions to be polarized. We note that electromagnetic radiation is comprised of traveling electric and magnetic fields that are perpendicular to each other, and also perpendicular to the direction of propagation. This is called a transverse wave. Polarization limits the types of oscillations in the fields that make up electromagnetic waves to a given direction or orientation. Linear polarization forces the electric field of the wave to oscillate along an axis, whereas circular polarization causes the electric field to rotate about an axis in the direction of travel, either counter-clockwise or clockwise. By observing the polarized radiation generated by the presence of a magnetic field in the star-forming regions where methanol masers are formed, astronomers can measure the strength of the magnetic field thereby getting a better idea of the stellar environment. The phenomena of observing the energy level splitting in the presence of external magnetic fields is known as the Zeeman Effect.

Methanol is a molecule with the largest quantity of known interstellar maser lines and has therefore been heavily documented. These various transitions originate from a substantial regime of energy levels above the ground state (also known as population inversion). By modeling the excitation of energy states, astronomers can extract crucial information on the early star-forming environments of higher mass stars and their properties.

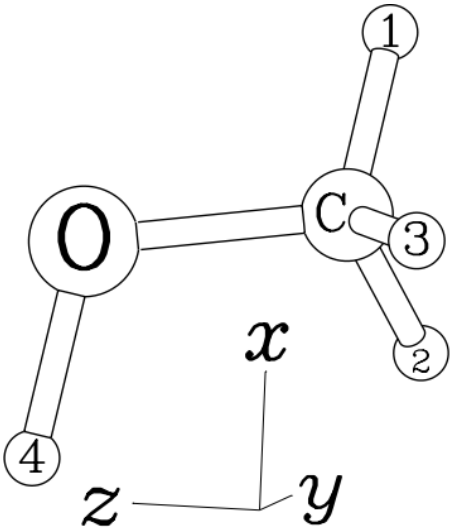

Figure 1: The methanol molecule represented in a Cartesian coordinate system (Coudert).

Figure 1 is a visual representation of the molecule, superimposed on a Cartesian coordinate plane, showing interatomic interactions, rotations, and geometry of methanol. The energy level splitting of the atoms in a

molecule is something we can observe associated with these interactions mentioned. Through the nuclei and electron quantum number states, we can observe the hyperfine structure, which is represented by the spectral data of a quantum system. The hyperfine structure differs from the fine structure, in that the latter accounts for electron spin magnetic moments and the orbital angular momentum of the electron. This hyperfine structure consists of the interactions of the magnetic moments of the nuclear spins of the protons in methanol. The C and O have nuclear spin = 0 (in their 12 and 16 isotopes). The protons interact with each other (dipole-dipole interactions), and with the overall rotation of the molecule, these are called spin-rotation interactions. The challenge with the hyperfine of methanol is that there exists an interaction of the magnetic moments of the proton with the torsion of methanol. The torsion of a molecule can be thought of as the counter-rotational twisting about the bond as a result to applied torque, generated by the rotational movement of atoms about a bond. A reason for structural inquiry of the methanol molecule, is its significant sensitivity to variations of the electron-proton mass ratios in the torsion-rotational structure. This sensitivity is strengthened by the torsional motion about the bonds. This enhancing effect is described as an interaction of the nuclear spins and are isotope dependent. This effect interacts with the magnetic field that is generated by the dynamic movement of methanol in the interstellar clouds around stellar environments.

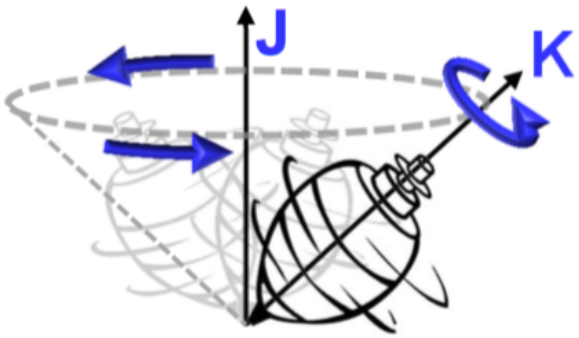

Figure 2: The spinning top model displaying the angular momenta of a symmetric top molecule (Hanson).

Figure 2 describes a symmetric top geometry and displays two angular momenta J and K. These quantum numbers account for the total angular momentum (J) and the angular momentum about the internuclear axis (the CO bond in methanol), describing the rotational energy levels of a molecule for a symmetric top. While methanol is an asymmetric top, this forms the groundwork for approximating the rotational energy levels for this molecule (Hanson). More specifically, methanol is a prolate, slightly asymmetric top and rotor molecule, which means that the principal moments of inertia are not equal along the three orthogonal axes. Due to the differences in electronegativity across the molecule, there exists a permanent electric dipole moment which gives rise to its unique spectra. The asymmetries are displayed by the difference in the distance between the hydroxyl (OH) protons and each of the methyl (CH_3) protons. The OH group is linear and off the axis of symmetry with respect to the CO bond, and the CH_3 group is tetrahedral in bonding structure. This molecule has numerous allowed transitions in the radio-wave regime of the electromagnetic spectrum.

Aspects of Group Theory can be applied to the understanding of the molecular geometry. There are symmetry operations, where indistinguishability before and after the operation persists, *e.g.,* rotation over an axis or plane of symmetry. There exists a categorical approach to the understanding of how a molecule can behave spatially in a given coordinate system. This can be done mathematically with matrix operations. (Hanson). Specifically with methanol, there are two types of symmetry, and they deal with energy transitions due to interatomic phenomena. They are designated as *A* and *E*, and are subject to different selection rules with a key difference in that transition of the *A*-type species involve an *A* +/- state that describes the parity of the spatial symmetry. The actual transitions deal with the total angular momentum quantum number travelling from the first state to the second, depicted as: $J_{Ka} \rightarrow J_{Kb}$ (in asymmetric top notation). The subject of these symmetries are the hydrogen spins of the CH_3 group, where in *A* and *E* methanol they are parallel and not parallel, respectively. There are no allowed radiative or collisional transitions between *A* and *E* type methanol because the nuclear spins interact

weakly with the rotation of the molecule and the electric field (Coudert).

METHODS

One of the objectives of our summer project was to compile a database of all the observed methanol maser transitions, with the longer term goal being to learn about the morphology of maser transitions in high-mass star-forming regions. The primary paper of inspiration for this literature inquiry was the 2018 paper by B. Lankhaar et al. This paper highlights the difficulty in experimentally analyzing methanol's magnetic characteristics, but instead provides a successful theoretical option that shows agreement with observational data. We sought to organize known methanol data in one place with the dual purpose of providing a place for ease of access/reference for future modeling and comparison, and to also provide a basic idea for maser morphology characterization through a hypothetical example. This example was based on what was learned in this literature search. In order to fulfill the narrower objective of compiling this list, previously discovered methanol maser lines were searched for in the literature through the SAO/NASA Astrophysics Data System (ADS). The search criteria pertained masers in star-forming regions and the appropriate frequencies for known methanol maser transitions, in addition to learning more about the most popular methanol maser lines (6.7 GHz, 12.2 GHz, 36 GHz, and 44 GHz). This was followed by a search for more obscure, less discussed methanol maser lines to diversify the data collection and provide a more detailed map of methanol maser morphology to be done in future work.

RESULTS

Our search of the literature resulted in a total of seventy methanol maser lines, ranging from 0.834 GHz to 241.904 GHz. A list of the maser transitions is presented in Table A.1 in the Appendix. The maser transitions are listed in order of increasing frequency. Column 1 in Table A.1 gives the frequency, column 2 gives the class, column 3 provides the state transition, column 4 shows the rest energy and column 5 shows the corresponding source(s).

Astronomical data for maser lines between 156.488 GHz and 157.276 GHz were provided by Slysh et al., in which the radial velocities of the observed lines resemble other Class II masers in the following regions: W3(OH), 345.01 + 1.79, W48, and Cep A. They suggest that these masers, excited with higher radiation temperature than the popular 6.7 GHz and 12.2 GHz counterparts, could be tied to "cometary bow-shocks" or molecular outflows from the early star environments (Slysh, Appendix).

The majority of rest energies were provided through a compiled data table by Muller et al. In addition, Leurini et al. provided a literature compilation of many of the same masers (Leurini). The rest energies for the associated line transitions ranged from 0.000 cm-1 to 243.031 cm-1, belonging to the 48.372 GHz ($1_0 \rightarrow 0_0 A^+$) and 296.37 GHz lines, respectively. Both of these lines are Class I methanol masers (Muller). In addition, they also classified a 24.928 GHz Class I maser and original maser lines ranging from 84.521 GHz to 108.893 GHz, which included both classes of masers (Appendix).

Cragg et al., provided an investigation in the 85-115 GHz frequency range for Class II maser sources of emission (Table 1). The ATNF (Australia Telescope National Facility), Mopra radio telescope, and SEST (Swedish-ESO Submillimeter Telescope) antennas were used. They concluded that there was evidence of three new lines in G345.01 + 1.79 region (RA 16 53 19.69, Dec. -40 09 46.0). These maser lines are cited in Table 1.

The most prominent methanol masers observed so far in the literature, indicated by "*" in Table A.1, are the Class II 6.7 GHz and 12.2 GHz lines and the Class I 36 GHz and 44 GHz lines (Table 1 & Appendix). The associated rest energies of these transitions are 33.786 cm-1, 13.556 cm-1, 18.803 cm-1, and 6.1380 cm-1, respectively.

Maser Line	Class	$J_{Ka} \rightarrow J_{Kb}$
6.7 GHz	II	$5_1 \rightarrow 6_0A^+$
12.2 GHz	II	$2_0 \rightarrow 3_{-1}E$
36 GHz	I	$4_{-1} \rightarrow 3_0E$
44 GHz	I	$7_1 \rightarrow 6_0A^+$
85.5 GHz	II	$6_{-2} \rightarrow 7_{-1}E$
86.6 GHz	II	$7_2 \rightarrow 6_3A^-$
86.9 GHz	II	$7_2 \rightarrow 6_3A+$

Table 1. Methanol maser lines with the corresponding class and rotational state transition ($J_{Ka} \rightarrow J_{Kb}$), which is standard asymmetric top notation (Muller, Leurini, Kalesnkii, Cragg).

Many of the known transitions for the methanol masers were compiled from publications with the following criteria: associated frequency lines, the corresponding transitions between rotational quantum number (J) levels, and rest energies. The aim was to grasp a better understanding of what high angular resolution lines in these transitions tell us about the position of Class I and II methanol masers with respect to each other. Missing data, indicated by "?," from the compiled data table (Appendix) are a result from inconclusive or unprovided data available in the sources investigated.

This literature search provided a way to organize both well documented and less common maser lines, which allowed a cohesive assessment of methanol morphology when coupled together with new data. While this list is not entirely exhaustive of all possible maser line transitions, the most important aspects of such a compendium is to plot each of these methanol masers against one another. This gives a collective map of maser morphologies, and provides a starting point for theoreticians to reference in data usage and comparison. This compilation would also benefit our own future work in understanding the Zeeman Effect.

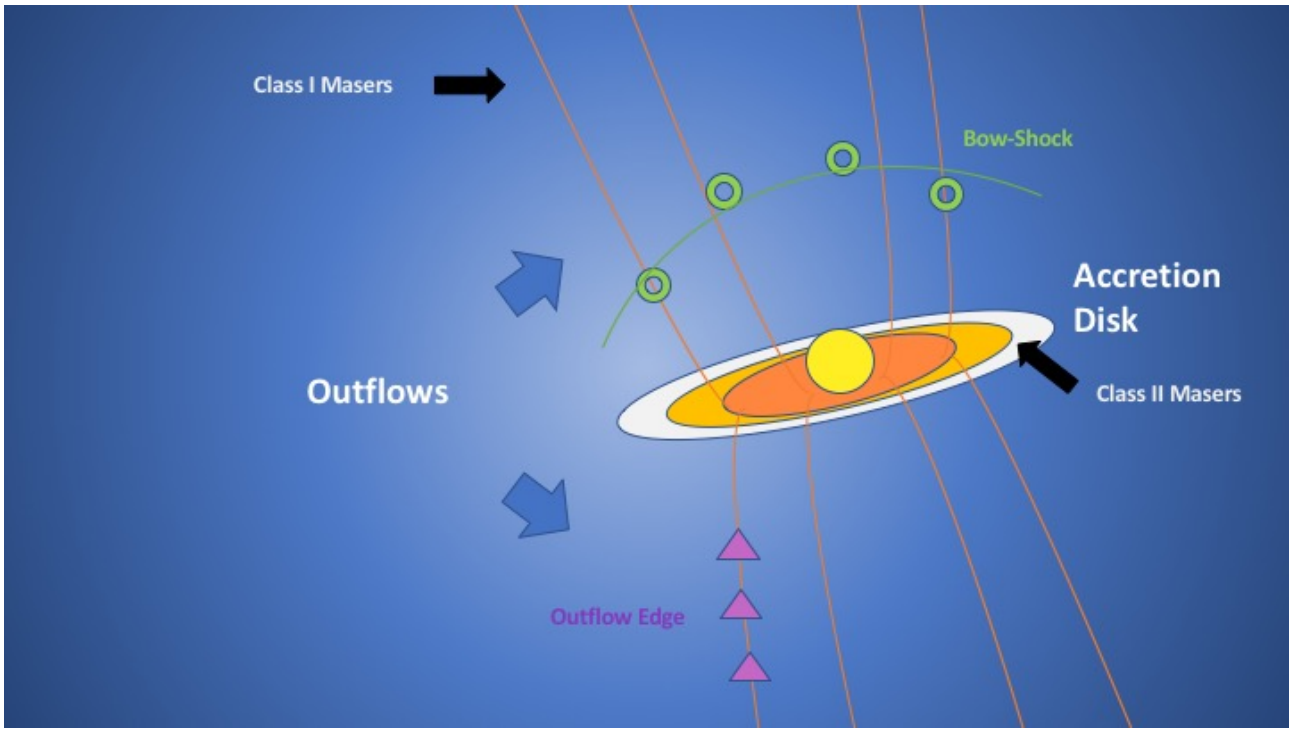

Figure 3: A hypothetical representation of using catalogued methanol maser lines for morphology identification in protostellar regions of sky.

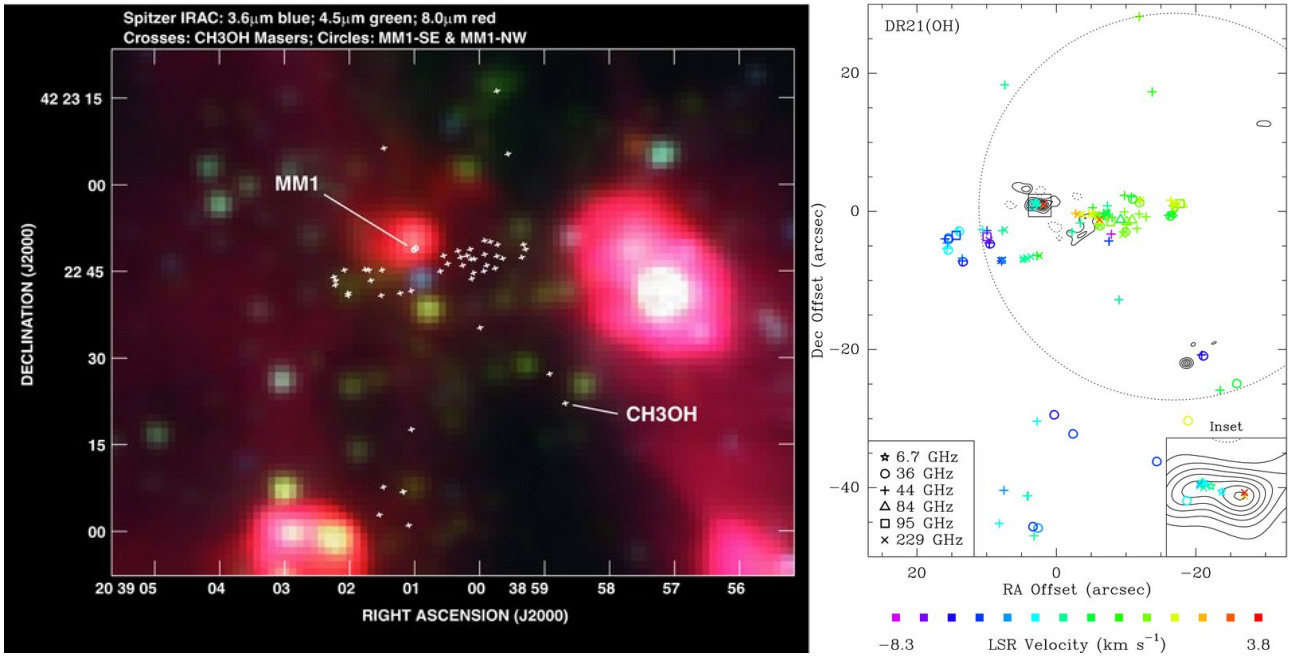

Figure 4: (Left) A near infrared image of the 44GHz Class I Methanol Maser from the Spitzer database (Araya 2009). (Right) A methanol masers plot including a Class II 6.7 GHz maser in the DR21(OH) Region (Fish 2011).

DISCUSSION

In order to help establish new morphologies of these methanol masers or to better understand those previously determined, we produced a catalogue of many known methanol masers. A catalogue can be an effective tool for morphological identification of these masers. This compilation of maser lines can allow researchers to pinpoint masers that are sufficiently bright and high intensity in order to measure the Zeeman Effect of these masers. This can be done through powerful telescopes like the VLA (Very Large Array).

The implications of similar masses of data include organized, future analysis of these masers in their protostellar environment, which can lead to a better understanding of the methanol molecule and how it interacts with the magnetic fields around young stars, leading to an increased understanding in high-mass star development. A hypothetical example is provided in Figure 3, displaying an artistic rendition of a protostellar environment and its key regions. This figure displays two sample morphologies: Bow-shocks (in green rings) and outflow edges (in magenta triangles). These characteristics of masers can be identified through studying the doppler-shifted velocities of real data. References to previously discovered data allow a cross-examination when plotting maser positions and obtaining distances between the maser hotspots to get a sense of their characteristics.

A concrete example in literature, in which such an approach has been used to analyze the maser morphology, but through real sky data was done by Araya *et al.* In analyzing the DR21(OH) region, the team was able to locate several masers, a group of which showed a class I 44 GHz line from the Spitzer database. This task was accomplished by looking at a range of Doppler shifted frequencies corresponding to velocities that arise as a result of the maser location relative to the galactic rotation. These masers can be pin-pointed to their physical source, based on those velocities. This represents the culmination of the hypothetical example proposed in this paper. A combination of literature data and a steady stream of new maser data can allow for complete assignment of certain stellar regions and thus a deeper understanding of the protostellar environments.

Figure 4 (left) displays class I methanol masers symbolized by crosses. The morphology of the blue-shifted (moving toward the observer) 44 GHz line in the DR21(OH) region can be described as a "bow-shock" (Araya). Visually, this is like the helm of a boat striding through ocean water. These morphologies are assumed in the literature to be outlining a younger evolutionary stage in the formation of this star. Figure 4 (right) includes the Class I and Class II, namely the 6.7 GHz line, methanol masers. In the main source region in DR21(OH), class I masers at 36 and 229 GHz are stacked over with class II 6.7 GHz, while also sharing the same velocity regime. Araya describes this as quite rare because these two classes are not typically found in the same space or subarcsecond. The dotted circle contains the primary maser beam for the 226 GHz lines and the 229 GHz maser observations. The box in the bottom right is an enlargement of the outlined box, where "6.7 GHz, 36 GHz, and 229 GHz masers appear to be in overlap" (Araya, Fish).

The energy levels in the torsion-rotation regime of the methanol molecule can comprise the astronomically observed masers. The hyperfine structure gets increasingly complicated with the torsion between the C and O atoms in the methanol molecule. The result is a much more complicated spectra, composed of the spinrotation, spin-torsion and spin-spin coupling. The magnetic moments of methanol are

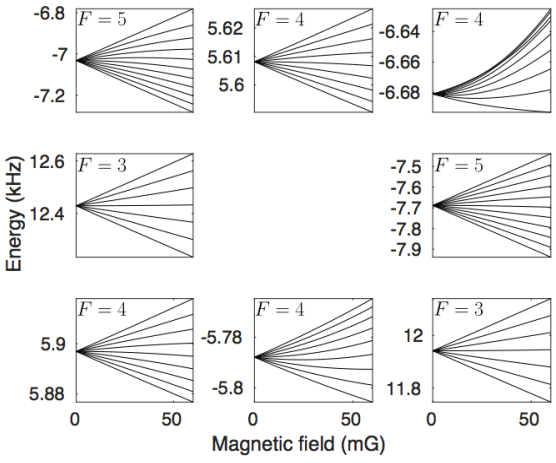

Figure 5: A plot showing energy and magnetic field strength to display the nonlinear dependence of Zeeman splitting in a magnetic field (Lankhaar).

responsible for these interactions and when in the external magnetic field of the violent environments of star formation, the Zeeman Effect can be observed through energy splitting determined by differences in energy spacing.

Figure 5 displays the non- lineardependence of Zeeman splitting in the presence of an external magnetic field. This is visualized by the bends in the slopes of energy against magnetic field strength. This effect is quite dependent on the strength of the magnetic field as well as the energy levels, as can be seen between diagrams. The quantum number F refers to a hyperfine interaction between the nuclear magnetic dipole moment and the magnetic field of electron spin, representing the total angular momentum of an atom with these effects accounted for. The relation between energy level and magnetic field will help describe the environments in these star-forming regions. This also ties back in the concept of radiative polarization, introduced previously (see Introduction), in that the detection of such polarized microwave radiation

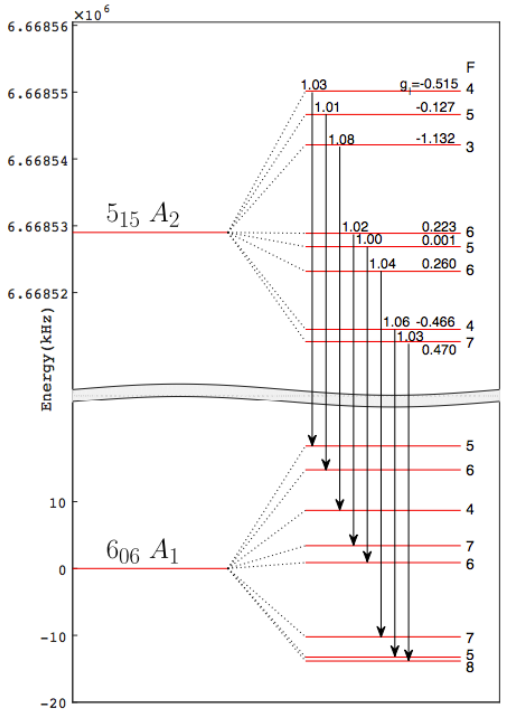

Figure 6: Energy level splitting as a result of the Zeeman Effect in rotational transitions of methanol

by intense methanol masers in the protostellar regions offer a direct link to better understanding the Zeeman Effect in methanol through a naturally occurring phenomenon.

In order to fully understand the hyperfine structure of the methanol molecule, and from that the magnetic field in the early star-forming environments, the Zeeman Effect is essential. Although not investigated in this paper, it is crucial for future work. In Figure 6, the Zeeman Effect can be visualized by the energy level splitting, where dashed lines show the new energy levels (right) generated by that splitting from the original energy level (left). The Zeeman Effect can be observed in the splitting of the rotational transitions of the methanol molecule. In order to grasp information from these spectra, the Zeeman Effect must be further understood, which is done by generating the Zeeman parameter, or net value, from the compilation of each individual splitting. However, the Zeeman parameters are unknown but crucial, as they allow observers to calculate the magnetic field based on these data types. Further cataloguing and mapping would lead to a better understand of this maser behavior in an early star-formation setting.

REFERENCES

Araya, E. D., Kurtz, S., Hofner, P., Linz, H. (2009). Radio continuum and methanol observations of DR21(OH). *The Astrophysical Journal*, *698*, 2.

Coudert, L. H., Gutle. C., Huet, T. R., Grabow, J. U., Levshakov, S. A. (2015). Spin-torsion effects in the hyperfine structure of methanol. *The Journal of Chemical Physics,* 143, 044304.

Cragg, D. M., Sobolev, A. M., Ellingsen, S. P., Caswell, J. (2001). Multitransition study and new detections of Class II methanol masers. *Monthly Notices of the Royal Astronomical Society*, *323, 4*, 939-95.

Fish, V. L., Muehlbrad, T. C., Pratap, P., Sjouwerman, L., Strelnitski, V., Pihlstrom, Y., Bourker, T. (2011). First interferometric images of the 36 GHz methanol masers in the DR21 complex. *The Astrophysical Journal*, *729*, 1.

Hanson, R. K. (2013). Quantitative laser diagnostics for combustion chemistry and propulsion, Lecture Notes, *Combustion Energy Frontier Research Center*, Princeton University.

Herbst, E., Sutton, E. C. (1984). Identification of the A and E hyperfine line ladders. *The Astrophysical Journal*, *333*, 2.

Kalenskii, S. V., Kurtz, S. (2016). A study of the region of massive star formation L379IRS1 in radio lines of methanol and other molecules. *Astronomy Reports, 60,* 702-717.

Lankhaar, B., Groenenboom, G. C., Avoird, A. (2016). Hyperfine interactions and internal rotation in methanol. *The Journal of Chemical Physics, 145, 2*.

Lankhaar, B., Vlemmings, W., Surcis, G., Langevelde, H., Groenenboom, G., Avoird, A. (2018). Characterization of methanol as a magnetic field tracer in star-forming regions. *Nature Astronomy*, *2,* 145–150.

Leurini, S. Schilke, P., Menten, K., Flower, D., Pottage, J., Xu, L. (2004). Methanol as a diagnostic tool of interstellar clouds. *Astronomy and Astrophysics, 422*, 573-585.

MPIA (2019). Physical and chemical conditions for high-mass star formation. *Max Planck Institute for Astronomy (MPIA)*.

Muller, H. S. P., Menten, K. M., Malder. H. (2004). Accurate rest frequencies of methanol maser and dark cloud lines. *Astronomy and Astrophysics*, *428*, 3.

Appendix: Table A.1 List of methanol maser transitions and data from literature.

Maser Line	Class	$J_{Ka} \rightarrow J_{Kb}$	Rest Energy	Reference
0.834 GHz	Class I	$1_1 \rightarrow 1_1 A^{\mp}$	11.705 cm^{-1}	Müller, H. S. P.,**2004**,*A&A* Radford, H. E. **1972**, *ApJ*, 174, 207 Ball, J. A.,**1970**,*ApJ*,168,L101
5.005 GHz	Class I	$3_1 \rightarrow 3_1 A^{\mp}$	19.703 cm^{-1}	Müller, H. S. P.,**2004**,*A&A* Robinson, B. J., **1974**, *Australian Journal of Physics*, 27, 865
*6.7 GHz	Class II	$5_1 \rightarrow 6_0 A^{+}$	33.786 cm^{-1}	Müller,H. S. P.,**2004**,*A&A* van der Walt, D. J.,**2007**,*A&A*,464,1015-1022 Menten, K. M. **1991**,*A& A*,198,253 Lankhaar, B., **2018**, *Nature Astronomy*, 2,145-150
9.936 GHz	Class II	$9_{-1} \rightarrow 8_{-2} E$	76.102 cm^{-1}	Müller, H. S. P.,**2004**,*A&A* Slysh, V. I., **1993**, *ApJ*, 413
*12.2 GHz	Class II	$2_0 \rightarrow 3_{-1} E$	13.556 cm^{-1}	Leurini, S.,**2004**, *A&A*,422,573-585 Pottage J. T.,**2001**, J. Opt. Phys., 34,3313 Haque, S. S.,**2001**, *The Astrophys. J.*,187,L15-17 Müller, H. S. P.,**2004**,*A&A* Batrla W., **1987**, *Nature*, 236, 49 Lankhaar, B., **2018**, *Nature Astronomy*, 2,145-150
19.967 GHz	Class II	$2_1 \rightarrow 3_0 E$	18.803 cm^{-1}	Müller, H. S. P.,**2004**,*A&A* Wilson, T. L., **1985**, *A&A*, 147, L19
23.121 GHz	Class II	$9_2 \rightarrow 10_1 A^{+}$	98.053 cm^{-1}	Müller, H. S. P.,**2004**,*A&A* Wilson, T. L., **1984**, *A&A*, 134, L7
24.928 GHz	Class I	$3_2 \rightarrow 3_1 E$	24.310 cm^{-1}	Müller, H. S. P.,**2004**,*A&A* Barrett, A. H., **1975**, *ApJ*, 198, L119
24.933 GHz	Class I	$4_2 \rightarrow 4_1 E$	30.764 cm^{-1}	Müller, H. S. P.,**2004**,*A&A* Barrett, A. H., **1971**, *ApJ*,168, L101 Gaines, L.,**1974**, *ApJ*, 191,L99
24.934 GHz	Class I	$2_2 \rightarrow 2_1 E$	19.469 cm^{-1}	Müller, H. S. P.,**2004**,*A&A* Barrett, A. H., **1975**, *ApJ*, 198, L119 Gaines, L.,**1974**, *ApJ*, 191,L99
24.959 GHz	Class I	$5_2 \rightarrow 5_1 E$	38.833 cm^{-1}	Müller, H. S. P.,**2004**,*A&A* Barrett, A. H., **1971**, *ApJ*,168, L101
25.018 GHz	Class I	$6_2 \rightarrow 6_1 E$	48.514 cm^{-1}	Müller, H. S. P.,**2004**,*A&A* Barrett, A. H., **1971**, *ApJ*,168, L101
25.125 GHz	Class I	$7_2 \rightarrow 7_1 E$	59.809 cm^{-1}	Müller, H. S. P.,**2004**,*A&A* Barrett, A. H., **1971**, *ApJ*,168, L101
25.294 GHz	Class I	$8_2 \rightarrow 8_1 E$	72.717 cm^{-1}	Müller, H. S. P.,**2004**,*A&A* Barrett, A. H., **1971**, *ApJ*,168, L101
25.541 GHz	Class I	$9_2 \rightarrow 9_1 E$	87.239 cm^{-1}	Müller, H. S. P.,**2004**,*A&A* Menten, K. M., **1986**, *A&A*, 157, 318
25.878 GHz	Class I	$10_2 \rightarrow 10_1 E$	103.373 cm^{-1}	Müller, H. S. P.,**2004**,*A&A* Matsakis, D. N., **1980**, *ApJ*, 236,481
26.847 GHz	Class I	$12_2 \rightarrow 12_1 E$	140.478 cm^{-1}	Müller, H. S. P.,**2004**,*A&A* Wilson, T. L., **1996**,*A&A*, 307, 209
27.472 GHz	Class I	$13_2 \rightarrow 13_1 E$	161.449 cm^{-1}	Müller, H. S. P.,**2004**,*A&A* Wilson, T. L., **1996**,*A&A*, 307, 209
28.169 GHz	Class I	$14_2 \rightarrow 14_1 E$	184.032 cm^{-1}	Müller, H. S. P.,**2004**,*A&A* Wilson, T. L., **1996**,*A&A*, 307, 209
28.906 GHz	Class I	$15_2 \rightarrow 15_1 E$	208.226 cm^{-1}	Müller, H. S. P.,**2004**,*A&A* Wilson, T. L., **1996**,*A&A*, 307, 209
28.969 GHz	Class II	$8_2 \rightarrow 9_1 A^{-}$	83.319 cm^{-1}	Müller, H. S. P.,**2004**,*A&A* Wilson, T. L., **1996**,*A&A*, 307, 209

Maser Line	Class	$J_{Ka} \rightarrow J_{Kb}$	Rest Energy	Reference
29.637 GHz	Class I	$16_2 \rightarrow 16_1 E$	243.031 cm^{-1}	Müller, H. S. P.,**2004**,*A&A*
				Wilson, T. L., **1996**,*A&A*, 307, 209
30.308 GHz	Class I	$17_2 \rightarrow 17_1 E$	261.445 cm^{-1}	Müller, H. S. P.,**2004**,*A&A*
				Wilson, T. L., **1996**,*A&A*, 307, 209
*36 GHz	Class I	$4_{-1} \rightarrow 3_0 E$	18.803 cm^{-1}	Kalenskii, S. V.,**2016**,*Astronomy Reports*,60,702-717
				Haque, S. S.,**2001**, *The Astrophys. J.*,187,L15-17
				Müller,H. S. P.,**2004**,*A&A*
				Morimoto, M.,**1985**,*ApJ*,288,L11
				Lankhaar, B., **2018**, *Nature Astronomy*, 2,145-150
37.703 GHz	Class II	$7_{-2} \rightarrow 8_{-1} E$	61.930 cm^{-1}	Müller, H. S. P.,**2004**,*A&A*
				Haschick, A.D., **1989**,*ApJ*, 346, 330
37.703 GHz	Class II	$6_2 \rightarrow 5_3 A^+$	58.813 cm^{-1}	Müller, H. S. P.,**2004**,*A&A*
				Haschick, A.D., **1989**,*ApJ*, 346, 330
38.293 GHz	Class II	$6_2 \rightarrow 5_3 A^-$	58.813 cm^{-1}	Müller, H. S. P.,**2004**,*A&A*
				Haschick, A.D., **1989**,*ApJ*, 346, 330
*44(.07) GHz	Class I	$7_1 \rightarrow 6_0 A^+$	6.1380 cm^{-1}	Kalenskii, S. V.,**2016**,*Astronomy Reports*, 60,702-717
				Müller, H. S. P., **2004**, *A&A*
				Morimoto, M.,**1985**,*ApJ*,288,L11
				Lankhaar, B., **2018**, *Nature Astronomy*, 2,145-150
44(.03) GHz	Class I	$3_1 \rightarrow 2_{-2} E$	?	Splatalogue: http://www.cv.nrao.edu
48.372 GHz	Class I	$1_0 \rightarrow 0_0 A^+$	0.000 cm^{-1}	Müller, H. S. P.,**2004**,*A&A*,
48.376 GHz	Class I	$1_0 \rightarrow 0_0 E$	9.122 cm^{-1}	Müller, H. S. P., **2004**, *A&A*
84.5 GHz	Class I	$5_{-1} \rightarrow 4_0 E$	3.0830 cm^{-1}	Kalenskii, S. V.,**2016**,*Astronomy Reports*,60,702-717
				Haque, S. S., **2001**, *The Astrophys. J.*,187,L15-17
				Müller, H. S. P., **2004**, *A&A*
				Batrla, W. **1988**, *ApJ*,329,L117
86.616 GHz	Class II	$7_2 \rightarrow 6_3 A^-$	68.493 cm^{-1}	Müller, H. S. P.,**2004**,*A&A*
				Sutton, E. C., **2001**,*ApJ*, 554, 173
86.903 GHz	Class II	$7_2 \rightarrow 6_3 A^+$	68.493 cm^{-1}	Müller, H. S. P.,**2004**,*A&A*
				Sutton, E. C., **2001**,*ApJ*, 554, 173
95.2 GHz	Class I	$8_0 \rightarrow 7_1 A^+$	7.2211 cm^{-1}	Kalenskii, S. V.,**2016**,*Astronomy Reports*,60,702-717
				Müller, H. S. P., **2004**,*A&A*
				Plambeck, R. L. **1988**, *ApJ*, 330, L61
96.739 GHz	Class I	$2_{-1} \rightarrow 1_{-1} E$	?	Leurini, S., **2004**, *A&A*,422,573-585
96.741 GHz	Class I	$2_0 \rightarrow 1_0 A$	?	Leurini, S., **2004**, *A&A*,422,573-585
96.744 GHz	Class I	$2_0 \rightarrow 1_0 E$	?	Leurini, S., **2004**, *A&A*,422,573-585
96.755 GHz	Class I	$2_1 \rightarrow 1_1 E$	?	Leurini, S., **2004**, *A&A*,422,573-585
104.300 GHz	Class I	$11_{-1} \rightarrow 10_{-2} E$	106.779 cm^{-1}	Müller, H. S. P.,**2004**,*A&A*
				Voronkov, M. A., **2004**, Proc. of European Workshop on Astronomical Molecules, 17-20
107.014 GHz	Class II	$3_1 \rightarrow 4_0 A^+$	16.134 cm^{-1}	Müller, H. S. P.,**2004**,*A&A*
				Val'tts, I. E., **1995**, *A&A*, 294, 825
108.894 GHz	Class II	$0_0 \rightarrow 1_{-1} A^+$	5.490 cm^{-1}	Müller, H. S. P.,**2004**,*A&A*
				Val'tts, I. E., **1999**, *MNRAS*, 310, 1077
132.891 GHz	Class I	$6_{-1} \rightarrow 5_0 E$	33.316 cm^{-1}	Müller, H. S. P.,**2004**,*A&A*
				Slysh,V.I.,**1997**,*ApJ*, 478, L37
146.619 GHz	Class I	$9_0 \rightarrow 8_1 A^+$	67.679 cm^{-1}	Müller, H. S. P.,**2004**,*A&A*
				Menten, K. M. **1991b**, Astronomical Society of the Pacific,119
156.489 GHz	Class II	$8_0 \rightarrow 8_{-1} E$	61.930 cm^{-1}	Müller, H. S. P.,**2004**,*A&A*
				Slysh,V.I.,**1995a**,*ApJ*,442, 668

Maser Line	Class	$J_{Ka} \rightarrow J_{Kb}$	Rest Energy	Reference
156.602 GHz	Class II	$2_1 \rightarrow 3_0 A^+$	9.681 cm^{-1}	Müller, H. S. P.,**2004**,*A&A*
				Slysh,V.I.,**1995a**,*ApJ*,442, 668
156.829 GHz	Class II	$7_0 \rightarrow 7_{-1} E$	49.035 cm^{-1}	Müller, H. S. P.,**2004**,*A&A*
				Slysh,V.I.,**1995a**,*ApJ*,442, 668
157.048 GHz	Class II	$6_0 \rightarrow 6_{-1} E$	37.749 cm^{-1}	Leurini, S., **2004**, *A&A*,422,573-585
				Müller, H. S. P.,**2004**,*A&A*
				Slysh,V.I.,**1995a**,*ApJ*,442, 668
157.179 GHz	Class II	$5_0 \rightarrow 5_{-1} E$	28.073 cm^{-1}	Leurini, S., **2004**, *A&A*,422,573-585
				Müller, H. S. P.,**2004**,*A&A*
				Slysh,V.I.,**1995a**,*ApJ*,442, 668
157.246 GHz	Class II	$4_0 \rightarrow 4_{-1} E$	20.009 cm^{-1}	Leurini, S., **2004**, *A&A*,422,573-585
				Müller, H. S. P.,**2004**,*A&A*
				Slysh,V.I.,**1995a**,*ApJ*,442, 668
157.270 GHz	Class II	$1_0 \rightarrow 1_{-1} E$	5.490 cm^{-1}	Leurini, S., **2004**, *A&A*,422,573-585
				Müller, H. S. P.,**2004**,*A&A*
				Slysh,V.I.,**1995a**,*ApJ*,442, 668
157.272 GHz	Class II	$3_0 \rightarrow 3_{-1} E$	13.556 cm^{-1}	Leurini, S., **2004**, *A&A*,422,573-585
				Müller, H. S. P.,**2004**,*A&A*
				Slysh,V.I.,**1995a**,*ApJ*,442, 668
157.276 GHz	Class II	$2_0 \rightarrow 2_{-1} E$	8.717 cm^{-1}	Leurini, S., **2004**, *A&A*,422,573-585
				Müller, H. S. P.,**2004**,*A&A*
				Slysh,V.I.,**1995a**,*ApJ*,442, 668
229.276 GHz	Class I	$8_{-1} \rightarrow 7_0 E$	54.266 cm^{-1}	Leurini, S., **2004**, *A&A*,422,573-585
				Müller, H. S. P.,**2004**,*A&A*
				Sastry, K. V. L. N., **1985**, *J. Mol. Spectrosc.*, 103, 486
				Slysh,V.I., **2002**,*Astronomy Reports*, 46, 49
241.700 GHz	Class ?	$5_0 \rightarrow 4_0 E$	?	Leurini, S., **2004**, *A&A*,422,573-585
241.767 GHz	Class ?	$5_{-1} \rightarrow 4_{-1} E$	?	Leurini, S., **2004**, *A&A*,422,573-585
241.791 GHz	Class ?	$5_0 \rightarrow 4_0 A$	?	Leurini, S., **2004**, *A&A*,422,573-585
241.806 GHz	Class ?	$5_4 \rightarrow 4_4 A$	?	Leurini, S., **2004**, *A&A*,422,573-585
241.806 GHz	Class ?	$5_{-4} \rightarrow 4_{-4} E$	?	Leurini, S., **2004**, *A&A*,422,573-585
241.813 GHz	Class ?	$5_{-4} \rightarrow 4_{-4} E$	?	Leurini, S., **2004**, *A&A*,422,573-585
241.829 GHz	Class ?	$5_4 \rightarrow 4_4 E$	?	Leurini, S., **2004**, *A&A*,422,573-585
241.832 GHz	Class ?	$5_3 \rightarrow 4_3 A$	?	Leurini, S., **2004**, *A&A*,422,573-585
241.833 GHz	Class ?	$5_3 \rightarrow 4_3 A$	?	Leurini, S., **2004**, *A&A*,422,573-585
241.842 GHz	Class ?	$5_2 \rightarrow 4_2 A$	?	Leurini, S., **2004**, *A&A*,422,573-585
241.843 GHz	Class ?	$5_3 \rightarrow 4_3 E$	?	Leurini, S., **2004**, *A&A*,422,573-585
241.852 GHz	Class ?	$5_{-3} \rightarrow 4_{-3} E$	?	Leurini, S., **2004**, *A&A*,422,573-585
241.879 GHz	Class ?	$5_1 \rightarrow 4_1 E$	?	Leurini, S., **2004**, *A&A*,422,573-585
241.887 GHz	Class ?	$5_2 \rightarrow 4_2 A$	?	Leurini, S., **2004**, *A&A*,422,573-585
241.902 GHz	Class ?	$5_{-2} \rightarrow 4_{-2} E$	?	Leurini, S., **2004**, *A&A*,422,573-585
241.904 GHz	Class ?	$5_2 \rightarrow 4_2 E$	?	Leurini, S., **2004**, *A&A*,422,573-585